Trends in Applied Sciences Research

ISSN 1819-3579

Academic
Journals Inc.

www.academicjournals.com

Trends in Applied Sciences Research 6 (8): 813-831, 2011
ISSN 1819-3579 / DOI: 10.3923/tasr.2011.813.831

Voltage Regulation and Dynamic Performance of the Tunisian Power System with Wind Power Penetration

[1]Saïdi Abdelaziz, [1]Ben Kilani Khadija, [2]Bouchoucha Chokri and [1]Elleuch Mohamed
[1]Electric Systems Laboratory, National Engineering School of Tunis, BP. 37, Le Belvedère, Tunisia
[2]Tunisian Electricity and Gas Company, Tunisia

Corresponding Author: Ben Kilani Khadija, Electric Systems Laboratory, National Engineering School of Tunis, BP. 37, Le Belvedère, Tunisia

ABSTRACT

The Tunisian power transmission grid will accommodate a wind power pool composed of five wind farms dispersedly placed on the national territory and based on variable speed induction generators. This study investigated the impact of this wind energy penetration on voltage regulation and the grid dynamic performance. The study was based on bifurcation diagrams taking the wind generation as a bifurcation parameter and on time response simulations to grid disturbances. We have considered network faults such as wind farm disconnection events, three-phase short-circuits at a conventional bus and voltage dip faults applied at wind connection buses. The additional wind power generation has significantly improved voltage regulation, although over voltages have been observed. Grid dynamic performance has shown compliance to voltage ride through capabilities and may be enhanced by additional reactive supply.

Key words: Wind power, tunisian power system, grid connection requirements, voltage regulation

INTRODUCTION

Wind energy is incontestably the fastest worldwide growing energy producing technology in terms of yearly growth of installed capacity. According to the Global Wind Energy Council, the wind power installed capacity worldwide has reached 157, 9 GW by the year 2009, the leader countries in installed wind power being the USA (35 159 MW), Germany (25 777 MW), China (25104 MW), Spain (19 149 MW) and India (10 926 MW). The environmental nonpolluting advantage of this renewable energy became a key element for future energy policies in many countries where wind energy has been used not as a replacement, but rather as an auxiliary complement to conventional power sources (Di Marino, 2008).

In the North African region wind power development has gained a primary position in government's promotional energy programs. Since 1990, the Tunisian Electricity and Gas Company (STEG) together with the National Agency for Energy Conservation (ANME) have launched various wind energy projects searching for potential wind power sites. The first wind power station has started up in 2000 in the region of Sidi Daoud with only 10 MW, followed by a first extension of 9 MW in 2003 and a second extension of 35 MW in 2008 (Mehiri, 2010). The current 55 MW installed wind power is up to be further extended to 265 MW by the year 2012 (Nur Energie, 2010; Brand and Zingerle, 2010). Four additional wind farms sites have been announced dispersed in the north and the northwestern regions of the national territory as shown in Fig. 1. The wind farms

Fig. 1: Wind farms locations in the Tunisian network

are designated WF1, WF2, WF3, WF4 and WF5, labeled in decreasing order with respect to their installed wind capacities: 135 MW, 55 MW, 30 MW, 30 MW and 12 MW, respectively.

Wind power farms have generally different characteristics from conventional power stations. They are relatively small sized, geographically dispersed and not dispatchable in a conventional way. When connected to the transmission grid, technical concerns relate to active and reactive power controls efficiency (Eping *et al.*, 2005). For the Tunisian power system, the wind power penetration level amounts to about 13% of the total network installed generation. It is characterized by a disproportion in the system load where about 50% is held in the northern part of the country and therefore voltage regulation issues are of primary concern for the system operator (U.S. Commercial Service, 2010).

According to the grid codes, Doubly Fed Induction Generators (DFIGs) are mainly used in variable speed wind turbines for several reasons: improved power quality, optimum power extraction and power factor regulation. These characteristic may be them able to provide a mandatory voltage support during and after system disturbances and faults (Fault Ride Through capability) using rotor converters control (Li and Chen, 2008; Holdsworth *et al.*, 2003). However, DFIGs have some constraints to ride-through voltage off-peaks which generate high voltages and currents in the rotor circuit and the power converter could be damaged (Alboyaci and Dursun, 2008).

Many studies have shown that when wind power penetration is large with respect to the total power rating, transient stability, fault analysis and voltage stability may significantly be affected (Jauch *et al.*, 2007; Karapidakis, 2007; Ameli *et al.*, 2008; Boonchiam *et al.*, 2009; Slootweg, 2003; Samarasinghe, 2007). Jauch *et al.* (2007) and Karapidakis (2007) investigated the effects of wind power on the stability of the Nordic and Crete's power system, respectively. The analysis of

Karapidakis (2007) suggested that it is possible to achieve a high level wind power penetration without dynamic security problems, if conventional units dispose of adequate spinning reserves and fast frequency and voltage controls. The study of Boonchiam *et al.* (2009) carried the study on the voltage stability of the IEEE 14 bus system including wind farm generators in weak buses, maximum loading margins are determined by a PV analysis. In order to maintain stable operation and avoid over-speed of the induction generators, some control strategies using FACTS devices are proposed to improve stability margins.

The aim of this study is to evaluate the voltage regulation and dynamic performance of the Tunisian power system integrating five distributed wind farms of total capacity 265 MW. The voltage stability assessment is based on bifurcation diagrams with wind generation as a bifurcation parameter. The effect of reactive limits and the wind generation parameter on the voltage profile is simulated in the peak and off-peak load events. Network faults are simulated for wind farm disconnection events, three-phase short-circuits at conventional buses and voltage dip faults applied at wind connection buses. The results are discussed in terms of voltage regulation capability and dynamic performance at wind connection buses for compliance to Grid Connection Requirement standards.

GRID CODE REQUIREMENTS

Transmission system operators have issued grid codes and grid requirements for wind turbine connection. The main issues of these requirements are (Alboyaci and Dursun, 2008):

- Frequency and power control
- Voltage control and power factor
- Fault ride through capability

The grid connection requirements of wind farms to the grid in some countries such as Denmark, Germany, Scotland, Ireland and United Kingdom by have been studied by Alboyaci and Dursun (2008) and Christiansen and Johnsen (2006). Among the chosen Grid Codes is Germany due to the high penetration of wind power and due to the important wind power market.

According to this grid operator (Li and Chen, 2008) wind parks must maintain uninterrupted generation during and after network faults (Fault Ride Through capability) and support the network frequency and voltage. Low voltage ride through is particularly important to maintain the voltage stability, especially in areas with high wind power generation. If the wind turbine is not designed to attain these requirements and disconnects from the network during a grid fault, this may result in severe stability failures in the power system which could amplify the disturbance (Christiansen and Johnsen, 2006).

Figure 2 shows the requirements of the lowest voltage that wind farms have to withstand. It shows that each wind farm remains transiently stable and connected to the power system without tripping with a total fault clearance time of up to 150 msec. During the operating range of the wind farms, these types of faults must not result in instability or isolation from the power system. Furthermore, Fig. 2 shows that wind generator shall be capable of continuous operation until 15% of nominal voltage at the connection point. When the voltage is in the shaded area, the turbine should supply reactive power to the network in order to maintain grid restoration (Alboyaci and Dursun, 2008).

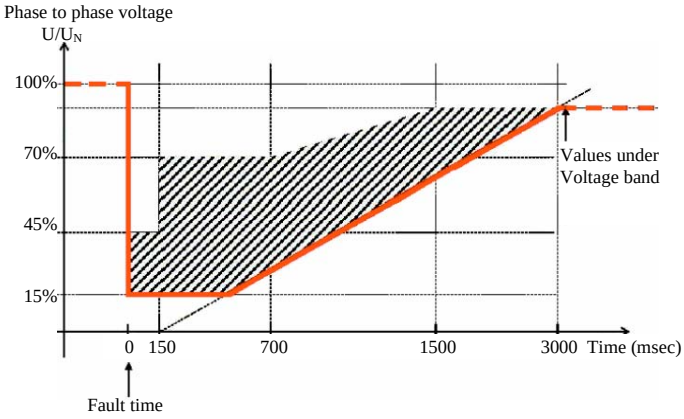

Fig. 2: Voltage off-peak that wind turbines should be able to handle without disconnection (E.On Netz) (Li and Chen, 2008)

SYSTEM MODELING

Network model: The transmission lines and transformers are represented by an equivalent π-circuit. At a bus i, the injected power equations may be written in the form:

$$P_i = \sum_{j=1}^{N} Y_{ij} V_i V_j \cos(\alpha_i - \alpha_j - \theta_{ij}) \quad (1)$$

$$Q_i = \sum_{j=1}^{N} Y_{ij} V_i V_j \sin(\alpha_i - \alpha_j - \theta_{ij}) \quad (2)$$

where, $\bar{V}_i = V_i \angle \alpha_i$ is the voltage at the ith bus, $\bar{Y}_{ij} = Y_{ij} \angle \theta_{ij}$ are the elements (i,j) of the network admittance matrix and N is the total number of network buses.

DFIG model: Using the generator convention, the machine equations of the DFIG written in a d-q synchronous reference frame are given by Ekanayake *et al.* (2003) and Ko *et al.* (2008). The stator voltages V_{sd} and V_{sq} are functions of the grid voltage magnitude V and phase θ at the DFIG bus:

$$V_{sd} = V_{sin}(-\theta) \quad (3)$$

$$V_{sq} = V_{cos}(\theta) \quad (4)$$

The electrical active and reactive powers generated by the stator are written as:

$$P_s = V_{sd} I_{sd} + V_{sq} I_{sq} \quad (5)$$

$$Q_s = V_{sq} I_{sd} + V_{sd} I_{sq} \quad (6)$$

where, I_{sd} and I_{sq} are the direct and quadrate stator currents. By choosing the d-q reference frame synchronized with the stator flux, the expressions of the active and reactive powers are given by Ghedamsi and Aouzellag (2010), Milano *et al.* (2007), Tsourakis *et al.* (2004) and Tsourakis *et al.* (2009).

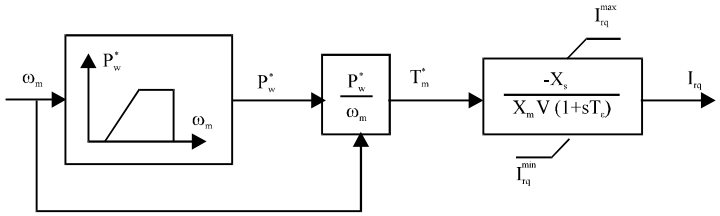

Fig. 3: Rotor speed control

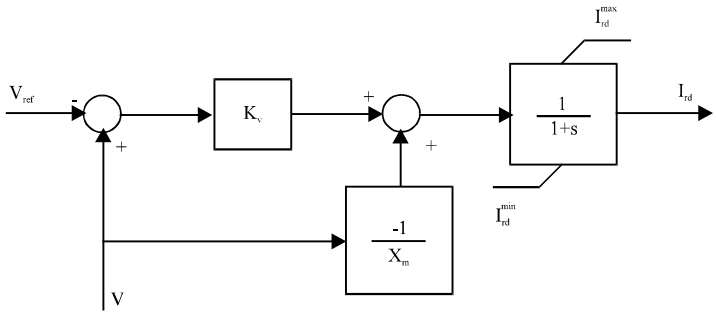

Fig. 4: Voltage control scheme

The mechanical motion equation is modelled as a single shaft, as it is assumed that the converter controls are able to filter shaft dynamics (Milano, 2005). The mechanical torque T_m extracted from the wind is:

$$T_m = \frac{P_w}{\omega_m} \tag{7}$$

where, ω_m is the rotor angular speed and P_w is the mechanical power function of the wind speed u_w and the blade pitch angle θ_p (Ghedamsi and Aouzellag, 2010).

Converter dynamics are highly simplified, as they are fast with respect to the electromechanical transients (Milano, 2008; Slootweg, 2003). Hence, the converter is modelled as an ideal current source where the rotor currents I_{rq} and I_{rd} are the state variables and are used for the rotor speed control and voltage control, respectively (Fig. 3, 4).

In Fig. 3 and 4, T_e is the power control time constant, K_v is the voltage control loop gain, V_{ref} is the reference voltage and $P_w^*(\omega_m)$ is the power-speed characteristic which roughly optimizes the wind energy capture and is calculated using the current rotor speed value (Fig. 5). It is noted that $P_w^* = 0$ if $1.3\ \text{p.u} \le \omega_m \le 0.7\ \text{p.u}$ and $P_w^* = 1$ if $1\ \text{p.u} < \omega_m \le 1.3\ \text{p.u}$. Thus, the rotor speed control has only an effect on subsynchronous speeds. Both the speed and voltage controls undergo antiwindup limiters in order to avoid converter overcurrents (Slootweg, 2003). Currents limits are used to define the active and reactive power generation limits which are as from (Milano *et al*., 2007). Consequently, DFIG models incorporate limited voltage control capabilities.

Finally, the pitch angle control is illustrated in Fig. 6 and described by the following differential equation:

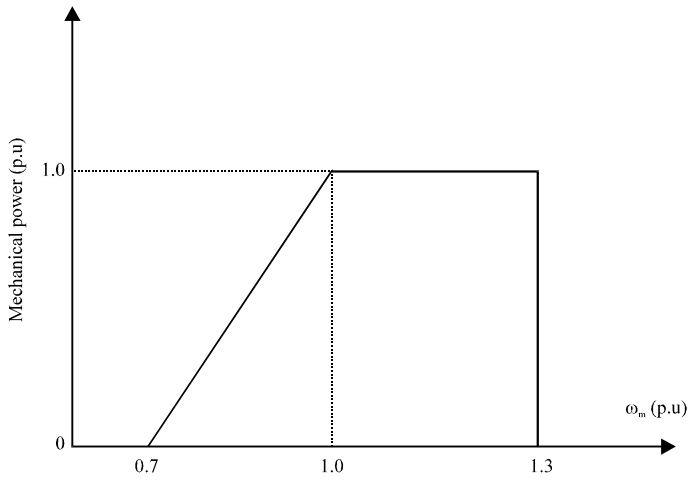

Fig. 5: Power-speed characteristic

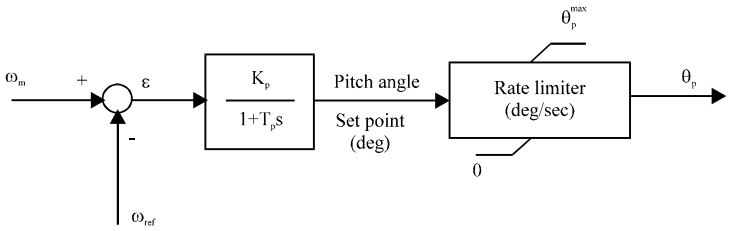

Fig. 6: Pitch angle control scheme

$$\dot{\theta}_p = \left(K_p \phi\left(\omega_m - \omega_{ref}\right) - \theta_p\right) / T_p \tag{8}$$

where, K_p and T_p are the gain and the time constant of the pitch control loop, respectively and Φ is the function that allows varying the pitch angle set point only if the difference $(\omega_m - \omega_{ref})$ exceeds a predefined value $\pm\Delta\omega$. The pitch control works only for supersynchronous speeds. An anti-wind up limiter locks the pitch angle to $\theta_p = 0$ for subsynchronous speeds.

THE CASE STUDY

Model description: Figure 7 depicts the 144-bus Tunisian transmission network. It comprises 144 buses, 30 generators, 67 loads, 67 transformers and 150 branches. The total system loading in the base case is 2800 MW and 1575 MVAR. The transmission grid operates at three voltage levels 225 kV, 150 kV and 90 kV. The synchronous generator buses are labeled G1 to G30, each generator is equipped with a Turbine Governor and an Automatic Voltage Regulator, the main power station of RADES (600 MW) is chosen as the slack bus (G6). The wind farms designated WF1, WF2, WF3, WF4 and WF5 are connected to buses 135, 143, 139, 142 and 137, respectively; the maximum installed wind power is 265 MW. Each wind farm comprises a number of wind generators, represented at their common point by one single equivalent wind turbine assuming homogeneous wind speed distribution in the wind farm (Akhmatov and Knudsen, 2002; Usaola *et al*., 2003) and operating with a power factor between 0.95 and 0.95 leading. The wind

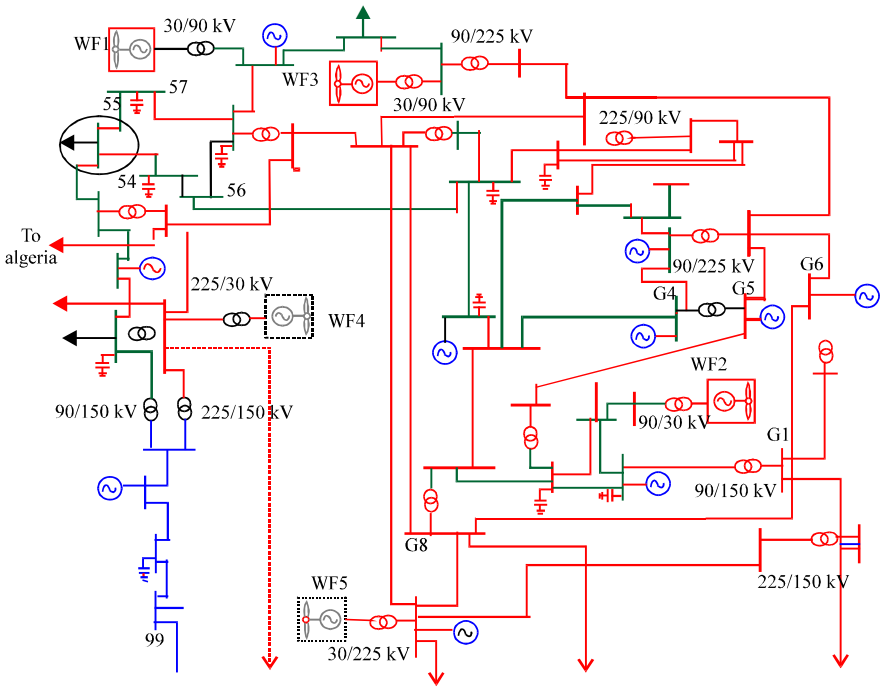

Fig. 7: Tunisian 144-bus transmission network: North area

Table 1: Wind turbine specifications

Variable	Description	Unit	Value
S_n	Rated power	MVA	100
V_n	Rated voltage	kV	30
f_n	Rated frequency	Hz	50
R_s	Stator resistance	p.u	0.01
X_s	Stator reactance	p.u	0.1
R_r	Rotor resistance	p.u	0.01
X_r	Rotor reactance	p.u	0.08
X_m	Magnetizing	p.u	3
H_m	Rotor inertia	sec	3
K_p	Pitch control gain	-	1
T_p	Pitch control time constant	s	3
K_v	Voltage control gain	-	10
T_c	Power control time constant	s	0.01
R	Rotor radius	m	75
p	Number of poles	int	4
n_b	Number of blades	int	3
η_{GB}	Gear box ratio	-	0.011236

turbine parameters are given in Table 1. The entire system has been implemented in MATLAB/PSAT toolbox (Milano, 2005) with system base values of 100 MVA, 30 kV and 50 Hz.

Steady state voltage: In load flow studies, DFIG wind turbines are commonly assimilated to PV type generator bus due to their active power generation and voltage control capability. When their reactive generation limits are reached, they are considered as load buses. We have represented each wind farm according to this hypothesis.

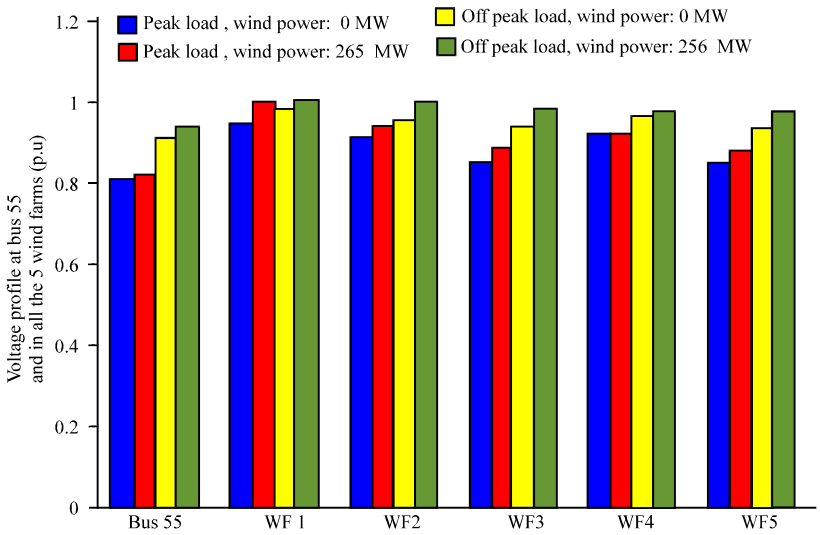

Fig. 8: Voltage profile with and without wind power in peak and off-peak load

We first tested the network voltage profile without and with wind power generation in peak and off-peak load conditions. This characteristic is depicted in Fig. 8. We note that with zero wind power, the wind farm connection buses low weak voltages, down to 0.84 p.u for WF3 and WF5 and only 0.81 p.u at bus 55. When all the 5 wind farms inject their max wind power, the voltage levels have increased at connection buses in the peak load condition. We further note that low voltage buses are located in the north western transmission grid (bus 55) which may be justified since the tie-connection to the neighbouring Algerian network are ignored in these simulations, no reactive support from the Algerian transmission grid which makes these buses weak. In the off-peak load and maximum wind power penetration, the simulations show no over-voltages. The voltage profile in the network and more particularly at the wind buses improved. The voltages in various buses of the network are contained in the acceptable tolerances of 10%.

Reactive power supply: Voltage control capability in a power system depends primarily on the overall available reactive power supply. In order to evaluate the contribution of the wind farms to voltage control, load flow simulations are used to generate the order in which generators reach their upper reactive generation limits (Q_g^{max}). In the event, they are converted to PQ-type buses in load flow calculations.

Figure 9 shows the generated sequence in the base case. Generator buses G10-12, G18-19, G24-25 and WF2-5 were initially PV type, reached their limits of reactive power generation. This sequence of generators depends on the loading condition, on the generator reactive capability and on the neighboring power sources. Conventional generator buses have been exhausted first and then came the wind farm generators. We note that, in all loading conditions, the larger size wind farm WF1 (135 MW) did not reach its reactive generation limits. For the next larger wind farm WF2 (55 MW), its reactive limits are reached in the peak loading case. The remaining wind farms WF3 (30 MW), WF4 (30 MW) and WF5 (12 MW) reach their reactive generation limits in the peak and the off-peak load and thus hardly contribute to the network voltage regulation. We also note the reactive power demand at WF3-5 in the peak load is high. This indicates that these wind connection buses suffer from insufficient reactive support.

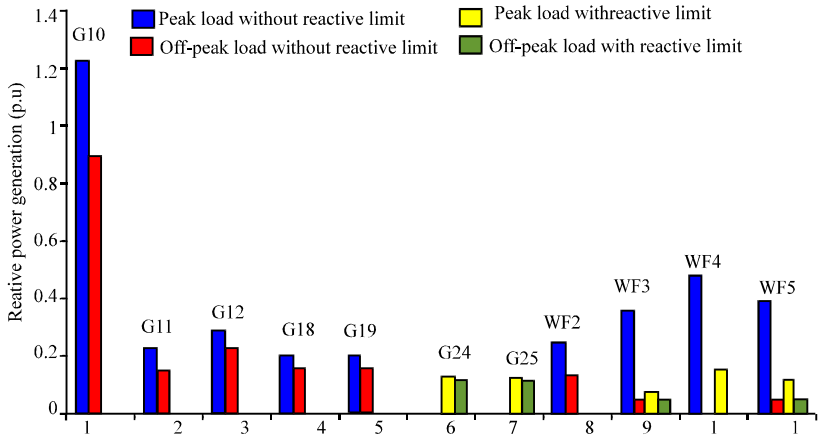

Fig. 9: Sequence of generators order reaching upper reactive generation limit in peak and off-peak load

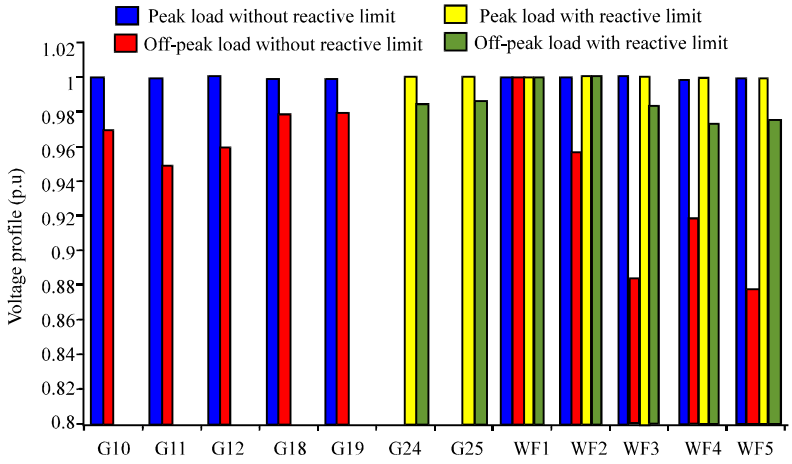

Fig. 10: Bus voltages with and without reactive limit in peak and off-peak load

Figure 10 simulates the effect of the reactive power limitation on the voltage profile. In the peak load we can see that the voltage at the wind farm WF1 is maintained to 1 p.u. On the other hand, despite the ability of the DFIG to regulate the power factor, voltages at the wind connections buses of WF3-5 are relatively low, these wind farms are of smaller size and their reactive control capability is accordingly limited.

Wind generation margin: Bifurcation diagrams are obtained taking wind power generation margin noted λ as a bifurcation parameter. We define λ as:

$$P_{gi} = \lambda_i P_g^{max} \tag{9}$$

where, P_g is the power generation by the DFIG wind farms.

Figure 11 shows the bifurcation diagram of voltage at bus 55 function of the wind generation margin in the peak-load case. In the first half of the curve, the voltage increases since the

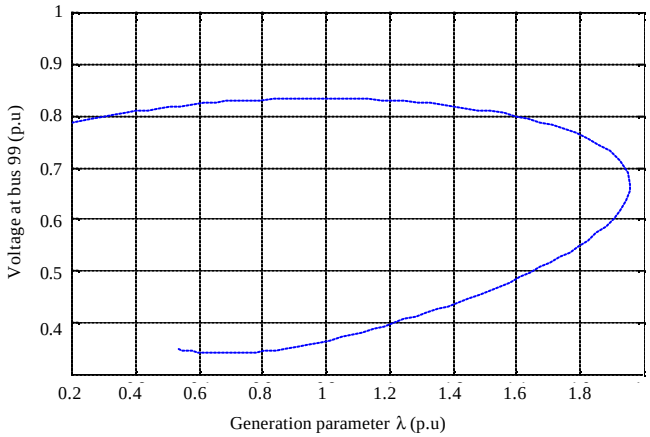

Fig. 11: Bifurcation diagram of voltage at bus 55 function in peak-load condition

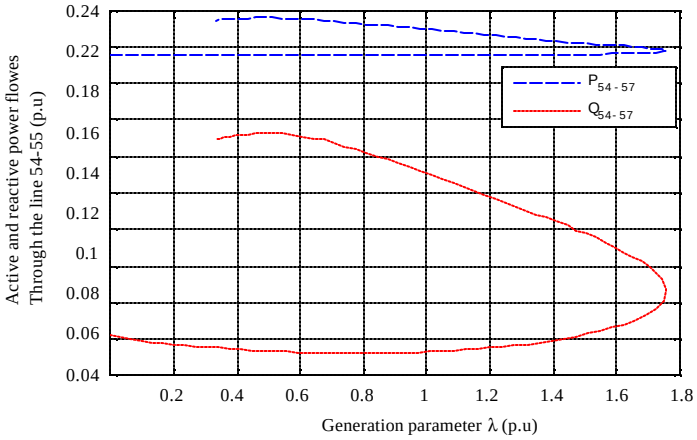

Fig. 12: Bifurcation diagrams of active and reactive power flows from bus 54 to bus 55 in peak load condition

distribution feeder is decreasing its power injection into the network when the generation parameter λ increases. In the second half of the curve, the voltage at bus 55 decreases which may be attributed to a power transfer limitation problem. The active and reactive power flows through the line 54-55 are simulated function of the wind generation parameter in Fig. 12. We can see that bifurcation occurs at the wind generation margin value of $\lambda = 1.8$ p.u. precisely at $\lambda_{max} = 1.7544$, the system collapses at a saddle-node bifurcation. This is the major contributing factor to voltage instability. The transmission system was up to be upgraded for high transmission capability. The maximum wind generation margin depends on the system loading condition. In the off-peak load case, the voltage collapse has occurred at the $\lambda_{max} = 2.073$ (Fig. 13). In this case, higher wind generation margin is allowed before reaching the bifurcation point. The bifurcation point is verified by the eigenvalue-locus shown in Fig.14 which depicts the change in minimum eigenvalues of the power flow Jacobian as the wind generation parameter increases. One eigenvalue crosses the imaginary axis for λ=1.7544 p.u., thus leading to a saddle-node bifurcation.

Time domain simulations of the voltage at bus 55 are illustrated in Fig. 15. We can observe that the system collapses at $t = 17$ sec when the wind generation parameter is $\lambda_{max} = 1.7544$ p.u.

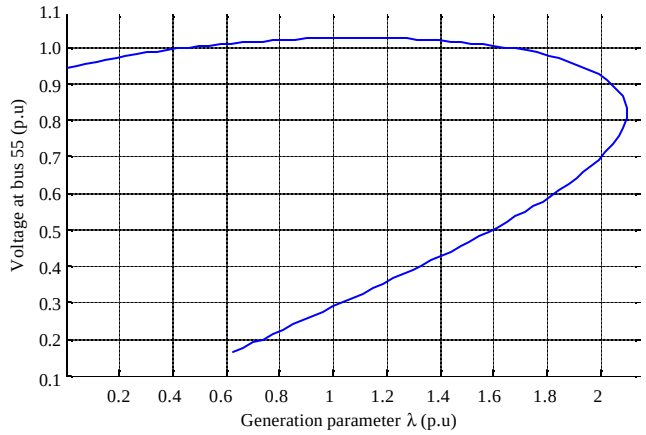

Fig. 13: Bifurcation diagram of voltage at bus 55 in off-peak load

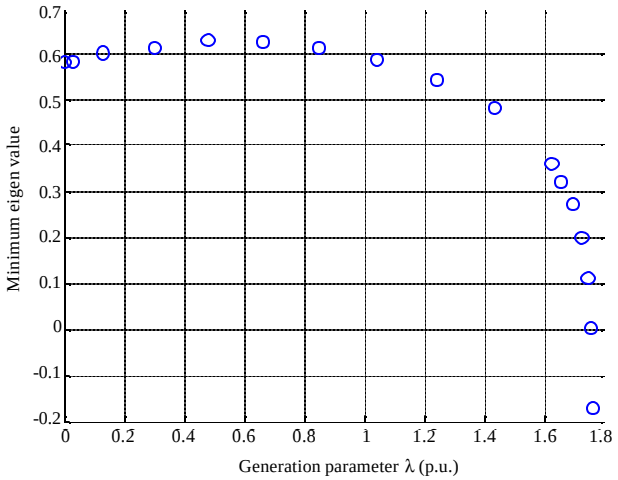

Fig. 14: Locus of minimum eigenvalue of the power flow Jacobian matrix

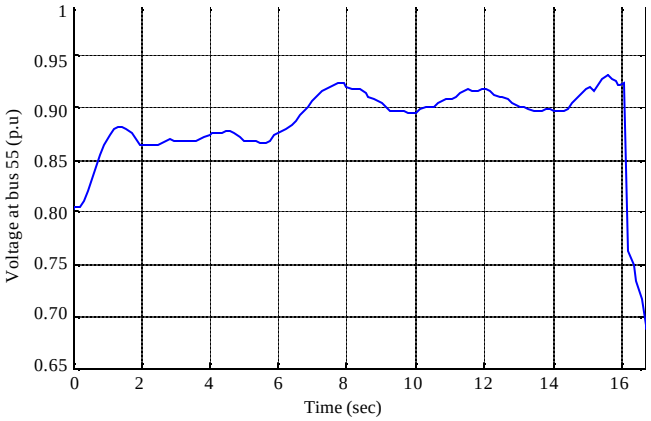

Fig. 15: Voltage magnitude at bus 55 for =1.7544 p.u

During this time the system attempts to compensate the line overloading conditions, the duration depends on the dynamic model of the induction generator which becomes unstable for a generation level close to 1.7544 p.u.

We further noted that with maximum wind penetration, voltage levels at bifurcation points were relatively higher. For example, the voltage profile at bus 99 is simulated function of the wind generation parameter in the peak-load case (Fig. 16), voltages close to the saddle node bifurcation were higher than 0.96 p.u. This implies that, the voltage collapse cannot be forecasted based only on voltage measures. This phenomenon is further prominent in the off-peak-load case.

Dynamic performance: The purpose of this section is to test the transient responses of the grid-connected wind generators and the synchronous network generators when a grid fault occurs. The system performances are analyzed for compliance to the grid requirement codes. For this purpose worst-case scenarios are considered. We first test the system transient response to a sudden wind power loss: disconnection of all wind farms. Then, three phase short circuit faults are applied at a regular transmission network bus (bus 55). Lastly, faulted voltage profiles are applied at the connection bus of the largest wind farm WF1.

In all the simulations, the initial conditions are a power output of 100% of the DFIG nominal power, corresponding to a wind speed of about 10 m sec^{-1} (Fig. 17).

Wind farm disconnection: All wind farms are abruptly disconnected from the network simultaneously by opening the circuit breakers. Immediately after the disconnection at t = 25 sec, as a result of the wind generation loss, the synchronous rotor speed of G6 dropped suddenly (swing bus) (Fig. 18). The steady state rotor speed is about 0.997 p.u corresponding to a frequency deviation of 150 mHz; noting that secondary control is desactivated in the simulations. The active power generation increased with a transient peak of 2.1356 p.u, the reactive power generation also increased from 1.4 p.u to 1.6 p.u as illustrated in Fig. 19. The synchronous machine turbine governor action lasted up to 4 seconds, after which the power oscillations are damped and the system retrieved its normal operation.

The disconnection causes a significant drop in the overall network voltage profile. In particular, for bus 55, the voltage decreased from 0.84 p.u to 0.79 p.u (Fig. 20).

Network short-circuit: We have chosen the network bus 55, as the faulted bus, since it has exhibited weak static voltage. A three-phase short circuit is applied at t = 15 sec, then cleared in 150 ms. The resulting voltage profiles are shown in Fig. 21. We can see a significant voltage drop at the wind connection WF3 reaching 0.85 p.u and at network buses nearby the faulted bus, reaching down to 0.5 p.u. Voltage regulation at this bus is assured since the DFIG has been extended by a fast, continuously acting controller in accordance with Fig. 4. A reactive power production of WF3 was depicted to provide voltage support during low voltage period which is shown in Fig. 23. The DFIG wind farms WF3, participate the most in supporting the network voltage. During the transient process, the effect of the fault on the DFIG wind farms WF1, WF2, WF4 and WF5 response is small. The response of the synchronous generator bus G6 is shown in

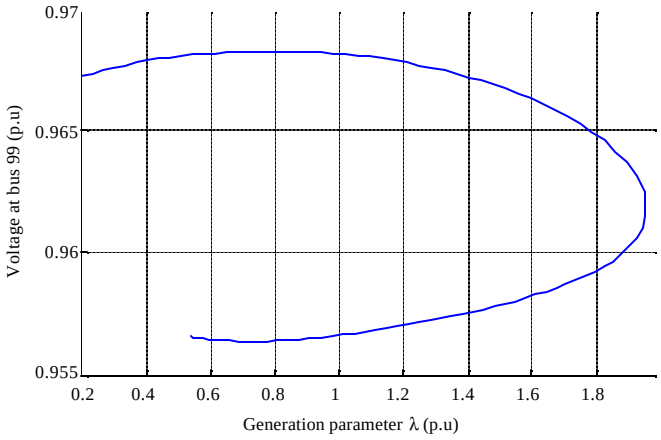

Fig. 16: Bifurcation diagram of voltage at bus 99 in peak-load

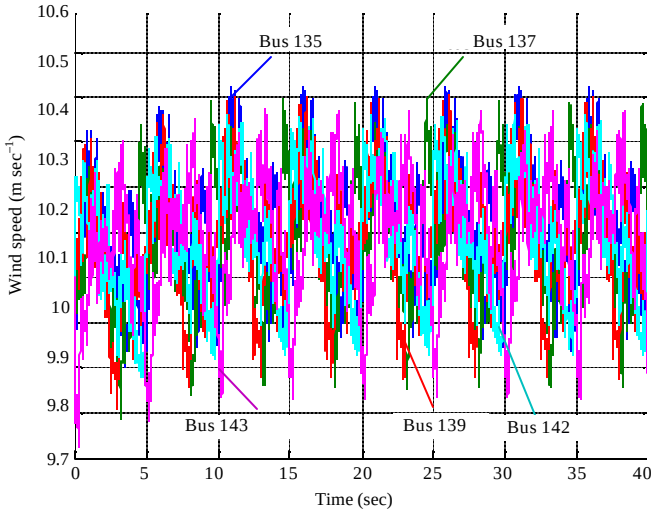

Fig. 17: Wind speed used for time domain simulation

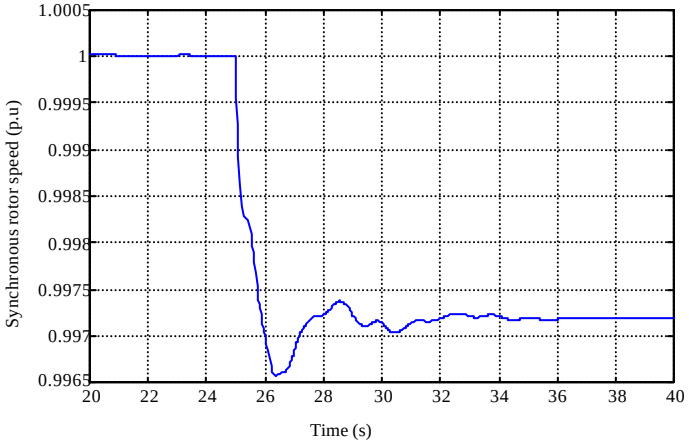

Fig. 18: Synchronous rotor speed of G6 after wind farms disconnection

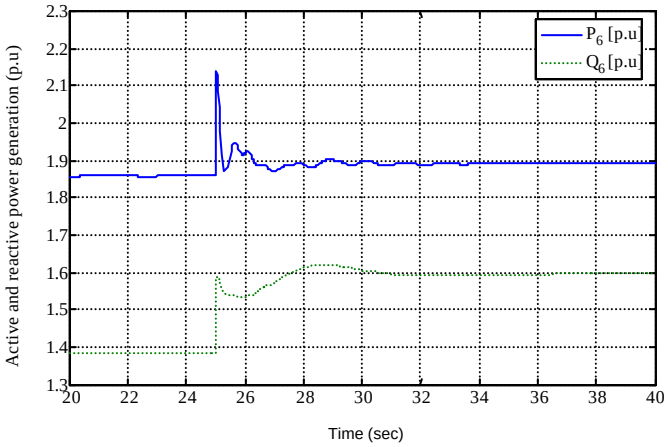

Fig. 19: Active and reactive generation at generator bus G6

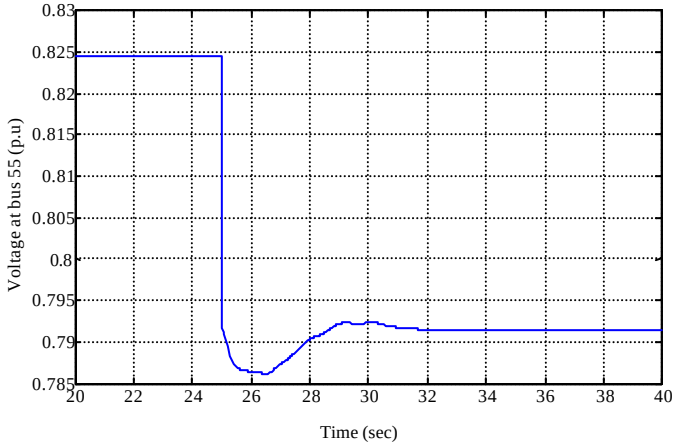

Fig. 20: Voltage at bus 55

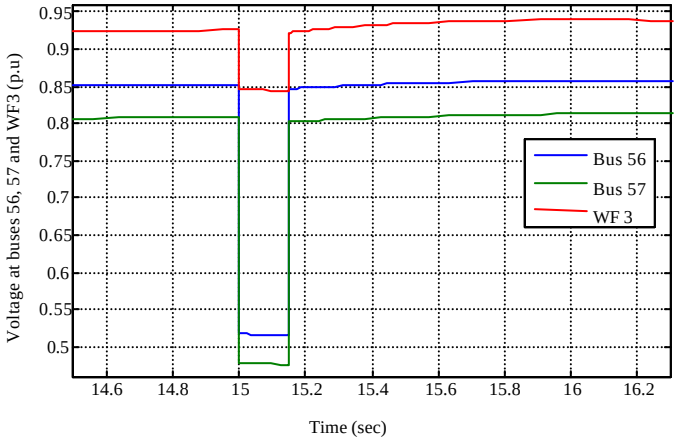

Fig. 21: Voltage at buses 56, 57 and WF3

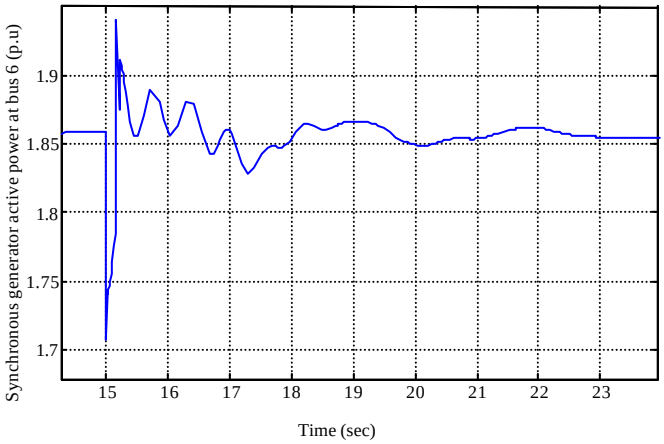

Fig. 22: Active power at the synchronous generator bus G6

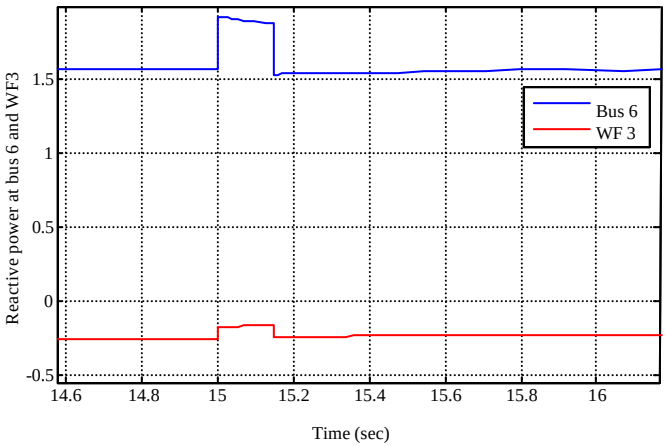

Fig. 23: Reactive power at the synchronous generator bus G6 and at WF3

Fig. 22 and 23. During the fault, the synchronous generator active power supply decreased and peak in the reactive power appears as the result of the short circuit.

Voltage dip faults at WF1: The system performance to transient three-phase voltage dips is assessed for compliance to the grid requirement codes. The reactive power requirements of wind farms are within a power factor of 0.95 to 0.95 leading. The fault voltage profiles are schematized in Fig. 24. The voltage dip occurs at 30 sec and lasts 150 ms with three voltage off-peak levels expressed in percent: h_1 = 72%, h_2 = 40% and h_3 = 7%. The fault is applied at the connection bus of the largest wind farm WF1. Figure 26-27 show the behaviour of the DFIG during the fault-ride through. Immediately after the fault occurs, the voltage at the wind turbine drops, the active power generation decreases and the reactive power increases.

Immediately after the fault is cleared at 30, 15 sec, as the DFIG begins a voltage regulation mode, the voltage at the wind turbine terminal starts to rise. As a result, the turbine

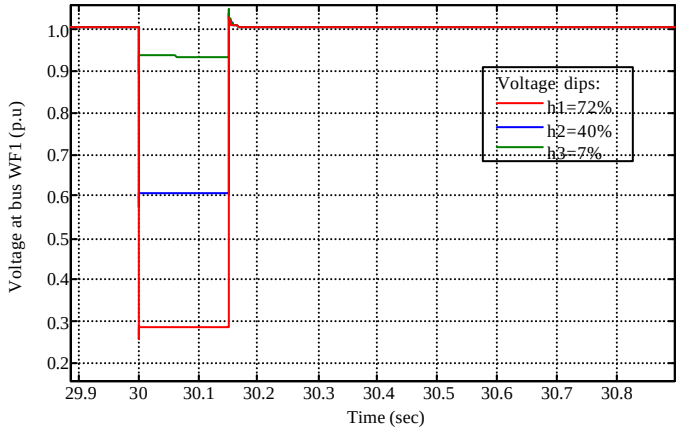

Fig. 24: Terminal voltage at WF1 for different voltage dips h1, h2, h3

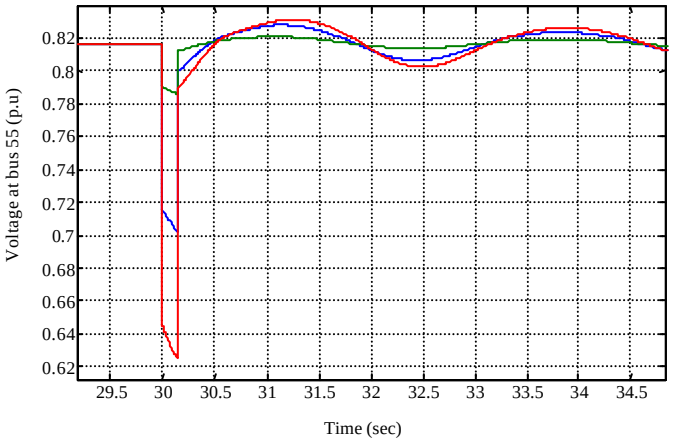

Fig. 25: Voltage at bus 55 for voltage dips h1, h2, h3 applied at WF1

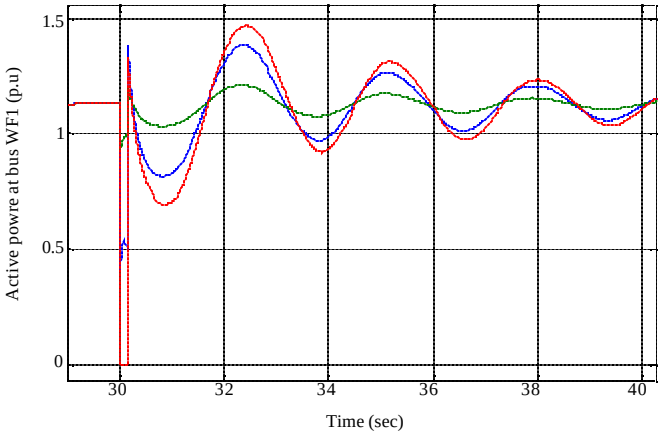

Fig. 26: Terminal active power at WF1 for different voltage dips h1, h2, h3

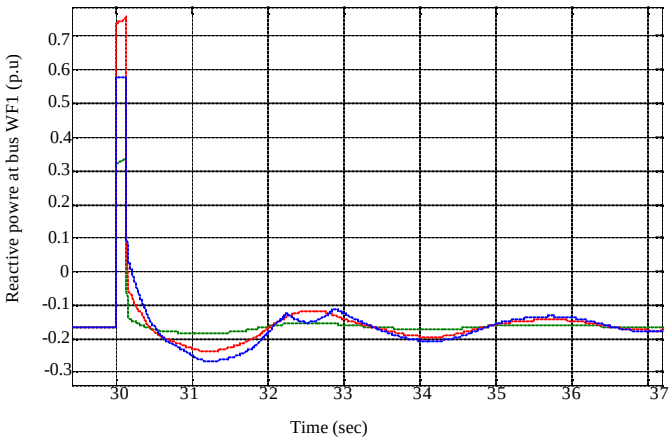

Fig. 27: Terminal reactive power at WF1 for different voltage dips h1, h2, h3

electromagnetic torque which is proportional to the voltage, increases instantly. The simulation results confirm that the wind turbine controllers are capable of re-establishing the voltage at the wind turbine terminal after the clearance of the short-circuit fault.

For the more serious fault corresponding to (h_1= 72%), the current flowing through the power converter may be too high which may cause damage to the rotor converter. In order to avoid such a risk, the DFIG is equipped with an over-current protection (Fig. 3-4). In case the rotor current magnitude reaches the setting value of the protection relay, the converter is blocked subsequently.

The voltage at bus 55 decreased significantly: 0.62 p.u for h_1, 0.70 p.u for h_2 and 0.78 p.u for h_3, as shown in Fig. 25. After the fault is cleared, the terminal voltage is recovered to the steady state value of 0.82 p.u.

CONCLUSION

This study investigated the voltage regulation and dynamic performance of the Tunisian power system integrating 265 MW wind energy. From the study and in comparison with the fixed speed wind turbine which needs capacitor bank for the reactive power compensation (Li and Chen, 2008) we noted a significant improvement in the system voltage regulation capability due to the additional capacity of absorption of reactive power offered by DFIG wind generators. In several researches (Linh, 2009; Li *et al.*, 2009; El-Kashlan *et al.*, 2005), the bifurcation diagram is based on the variation of the loading factor but in this paper we assume that the bifurcation parameter is the power generated by the dispersed wind farms. The bifurcation diagrams of voltages indicated that with high wind penetration, voltage bifurcation may occur at higher voltages. Voltage measures are not sufficient as a voltage instability indicator.

Wind farms abrupt disconnection has resulted in a frequency drop of 150 mHz and voltage drop 15% of the nominal voltage which affected mostly the North Western area of the country. Secondary frequency regulation action is necessary. The additional wind power generation has significantly improved voltage regulation, although over voltages have been observed. Grid dynamic performance has shown compliance to voltage ride through capabilities and may be enhanced by additional reactive supply.

Further refinement, such as including a two-masses shaft system used in the doubly fed induction generator would further improve the model.

ACKNOWLEDGMENTS

This work was supported by the Tunisian Ministry of High Education, Research and Technology. The authors would like to acknowledge all the help and contribution of the Tunisian Electricity and Gas Company (STEG) and also the reviewers for their helpful comments to this paper.

REFERENCES

Akhmatov, V. and H. Knudsen, 2002. An aggregate model of gird-connected, large scale, offshore wind farm for power stability investigations-importance of windmill mechanical system. Int. J. Electric Power Energy Syst., 24: 709-717.

Alboyaci, B. and B. Dursun, 2008. Grid connection requirements for wind turbine systems in selected countries-comparison to Turkey. EPQU Magazine, Vol. 3.

Ameli, M.T., S. Moslehpour and V. Sotudehnegad, 2008. Reducing the undesirable effects of wind farms high-penetration on frequency. Proceedings of the 2008 IAJC-IJME International Conference, ISBN: 978-1-60643-379-9. http://www.ijme.us/cd_08/PDF/239_ENG_108.pdf.

Boonchiam, P.N., A. Sode-Yome, N. Mithulananthan and K. Aodsup, 2009. Voltage stability in power network when connected wind farm generators. Proceedings of the International Conference on PEDS 2009 Power Electronics and Drive Systems, Nov. 2-5, Taipei, pp: 655-660.

Brand, B. and J. Zingerle, 2010. The renewable energy targets of the Maghreb countries: Impact on electricity supply and conventional power markets. EWI Working Paper, No. 10/02. May 2010. http://www.ewi.uni-koeln.de/fileadmin/user/WPs/ewiwp1002.pdf.

Christiansen, W. and D.T. Johnsen, 2006. Analysis of requirements in selected grid codes. Section of Electric Power Engineering, Technical University of Denmark (DTU). http://www.frontwind.com/Analysis%20of%20the%20requirements%20in%20selected%20Grid%20Codes.pdf.

Di Marino, E., 2008. Integrating large shares of fluctuating power sources into power electric systems: Impact on the development of distribution networks. Proceedings of the Infrastructure Network Division Enel-Italy, Aug. 25th, Paris, pp: 1-31.

Ekanayake, J.B., L. Holdsworth and N. Jenkins, 2003. Comparison of 5th order and 3rd order machine models for Doubly Fed Induction Generator (DFIG) wind turbines. Electr. Power Syst. Res., 67: 207-215.

El-Kashlan, S.A., M. Abdel-Rahman, H. El-Dessouki and M.M. Mansour, 2005. Voltage stability of wind power system using bifurcation analysis. A Scientific and Technical Publishing Company. http://www.actapress.com/Abstract.aspx?paperId=20772.

Eping, Ch., J. Stenzel, M. Poller and H. Muller, 2005. Impact of large scale wind power on power system stability. Proceedings of the 5th International Workshop on Large-Scale Integration of Wind Power and Transmission Networks for Offshore Wind Farms, April 2005, Glasgow, Scotland, pp: 1-9.

Ghedamsi, K. and D. Aouzellag, 2010. Improvement of the performances for wind energy conversions systems. Int. J. Electron. Power Energy Syst., (In Press).

Holdsworth, L., X.G. Wu, J.B. Ekanayake and N. Jenkins, 2003. Comparison of fixed speed and doubly-fed induction wind turbines during power system disturbances. Generation Transmission Distribution IEE Proc., 150: 343-352.

Jauch, C., P. Sorensen, I. Norheim and C. Rasmussen, 2007. Simulation of the impact of wind power on the transient fault behavior of the Nordic power system. Electr. Power Syst. Res., 77: 135-144.

Karapidakis, E.S., 2007. Transient analysis of crete's power system with increased wind power penetration. Proceedings of the International Conference on POWERENG, Power Engineering, Energy and Electrical Drives, April 12-14, Setubal, Portugal, pp: 18-22.

Ko, H.S., G.G. Yoon, N.H. Kyung and W.P. Hong, 2008. Modeling and control of DFIG-based variable-speed wind-turbine. Electric Power Syst. Res., 78: 1841-1849.

Li, H. and Z. Chen, 2008. Overview of different wind generator systems and their comparisons. IET Renew. Power Gener., 2: 123-138.

Li, X., Z. Zeng, J. Zhou and Y. Zhang, 2009. Small signal stability analysis of large scale variable speed wind turbines integration. Proceedings of the International Conference on Electrical Machines and Systems, Oct. 17-20, Wuhan, pp: 2526-2530.

Linh, N.T., 2009. Voltage stability analysis of grids connected wind generators. Proceedings of the 4th IEEE Conference on Industrial Electronics and Applications, May 25-27, Xi'an, pp: 2657-2660.

Mehiri, M., 2010. Development of the Tunisian power system and interconnections with neighbouring countries. Proceedings of the 8th Conference FEMIP, Conference Center of Valencia, May 10th, Spain, pp: 1-24.

Milano, F., 2005. Power system analysis toolbox documentation for PSAT. Version 1.3.4. http://www.power.uwaterloo.ca/~fmilano/psat.htm.

Milano, F., 2008. Assessing adequate voltage stability analysis tools for networks with high wind power penetration. Proceedings of the 3rd International Conference on Electric Utility Deregulation and Restructuring and Power Technologies, April 6-9, Nanjing, China, pp: 2492-2497.

Milano, F., A.J. Conejo and J.L. Garcia-Domelas, 2007. Reactive power adequacy in distribution networks with embedded distributed energy resources. J. Energy Eng., 133: 132-143.

Nur Energie, 2010. Nur energie CSP in North Africa. 12th April 2010, London, pp: 1-15. http://213.133.109.5/video/energy1tv/Jan%20NEU/Konferenz/Wirtschaft/DESERTEC_10/HMI_10/PPP/Till_Stenzel_Nur%20Energier_Tunisia.pdf.

Samarasinghe, C., 2007. Effect of wind generation on small disturbance voltage stability. Wind Generation Investigation Project, Transpower New Zealand Ltd., May 2007.

Slootweg, J.G., 2003. Wind power: Modelling and impact on power system dynamics. Ph.D. Thesis, Delft University of Technology, Delft, The Netherlands.

Tsourakis, G., B.M. Nomikos and C.D. Vournas, 2009. Effect of wind parks with doubly fed asynchronous generators on small-signal stability. Electr. Power Syst. Res., 79: 190-200.

Tsourakis, G., E. Potamianakis and C. Vournas, 2004. Eliminating Voltage Instability Problems in Wind Parks by using Doubly Fed Induction Generators. National Technical University of Athens, London.

U.S. Commercial Service, 2010. Doing business in Tunisia: 2010 country commercial guide for U.S. companies. International Copyright, U.S. and Foreign Commercial Service and U.S. Department of State, 2010. All Rights Reserved Outside of the United States.http://www.buyusa.gov/tunisia/en/doing_business_in_tunisia.pdf.

Usaola, J.L., P. Rodriguez, J.M. Fernandez, J.L. Beato, D. Iturbe and Jr. R. Wilhelmi, 2003. Transient stability studies in grids with great wind power penetration. Modelling issues and operation requirements. Power Eng. Soc. General Meeting, 3: 1534-1541.